applied sciences

MDPI

Article

PLA-Sago Starch Implants: The Optimization of Injection Molding Parameter and Plasticizer Material Compositions

Yudan Whulanza [1,2,*], Mohamad Taufiqurrakhman [3,*], Sugeng Supriadi [1,2], Mochamad Chalid [4], Prasetyanugraheni Kreshanti [5] and Athoillah Azadi [6]

1 Research Center for Biomedical Engineering, Faculty of Engineering, Universitas Indonesia, Kampus UI, Depok 16424, Indonesia; sugeng@eng.ui.ac.id
2 Department of Mechanical Engineering, Faculty of Engineering, Universitas Indonesia, Kampus UI, Depok 16424, Indonesia
3 Institute of Functional Surfaces (iFS), School of Mechanical Engineering, University of Leeds, Leeds LS2 9JT, UK
4 Department of Metallurgical and Material Engineering, Faculty of Engineering, Universitas Indonesia, Kampus UI, Depok 16424, Indonesia; chalid@metal.ui.ac.id
5 Plastic Reconstructive and Aesthetic Surgery Division, Department of Surgery, Cipto Mangunkusumo Hospital, Faculty of Medicine, Universitas Indonesia, Depok 16424, Indonesia; prasetyanugraheni@ui.ac.id
6 Indonesian Agency for Agricultural Research and Development, Jakarta 12540, Indonesia; athoillah@pertanian.go.id
* Correspondence: yudan.whulanza@ui.ac.id (Y.W.); menmtau@leeds.ac.uk (M.T.)

Abstract: Previous research extensively characterized PLA blends for various biomedical applications, especially in polymer-based biodegradable implant fixations, offering advantages over metallic counterparts. Nevertheless, achieving an optimal PLA mixture with both mechanical resistance and fast biodegradability remains a challenge. Currently, literature still lacks insights into the manufacturing parameter impact on sago starch/PLA in combination with PEG plasticizer. The objective of this study is to assess variations in injection molding temperatures and sago/PLA/PEG weight compositions to identify the optimal combination enhancing miniplate mechanical properties and biodegradation behavior. Mechanical tests reveal that incorporating PEG into pure PLA yields high mechanical performance, correlating linearly with increasing injection temperature. However, the interaction once the three materials are mixed decreases mechanical performance across tested temperatures. Higher biodegradation rates are observed with a larger weight composition of the hydrophilic behavior attributed to sago starch presence. The observed novelty in PLA mixed with 20% sago starch and 10% PEG at 170 °C indicates a better performance in elastic modulus and elongation at break also the degradation rate, emphasizing the role of injection temperature in molding miniplate implants. In conclusion, the interplay of injection molding parameters and material compositions is crucial for optimizing PLA-based miniplate implants, with potential contributions to tissue implants rather than bone implants due to their mechanical limitation.

Keywords: sago starch; degradable PLA; PEG plasticizer; degradable implant

Citation: Whulanza, Y.; Taufiqurrakhman, M.; Supriadi, S.; Chalid, M.; Kreshanti, P.; Azadi, A. PLA-Sago Starch Implants: The Optimization of Injection Molding Parameter and Plasticizer Material Compositions. *Appl. Sci.* **2024**, *14*, 1683. https://doi.org/10.3390/app14051683

Academic Editor: Manoj Gupta

Received: 31 December 2023
Revised: 2 February 2024
Accepted: 7 February 2024
Published: 20 February 2024

1. Introduction

In recent decades, the use of biodegradable implant fixations, including screws and plates for bone connections in fractures, has become increasingly common, particularly in applications like maxillofacial bone repairs [1–4]. These implants present notable advantages over their metallic counterparts, preventing the need for removal surgeries and facilitating unimpeded bone growth [5,6]. Furthermore, they mitigate long-term biohazards associated with metallic implants, such as corrosion, stress shielding-induced osteoporosis and adverse effects from medical imaging procedures like computer tomography scans and radiography [7]. Despite these benefits, challenges persist, including a rapid weakening in

tensile strength and potential mismatches in degradability rates. Ideally, implants should degrade as fractures regain structural integrity during the recovery and growth process, acknowledging that bone remodeling can occur within three months to two years [8,9]. Recent studies even suggest the remodeling starting as early as a month after a fracture, continuing beyond the typical two-month period [10]. In contrast, existing miniplate implants take approximately one to five years to degrade [5]. To address these challenges, new materials such as polylactic acid (PLA) have emerged, offering transient properties that commence with strength and support and gradually degrade over time, making space for newly grown bone to take over [11].

PLA stands out as the most commonly used biodegradable polymer in contemporary clinical applications [12]. Its versatility spans applications in drug delivery systems, tissue engineering and both temporary and permanent implantable devices, continually expanding into new fields [6]. This widespread use is attributed to PLA's favorable biocompatibility and the production of safe degradation devices, making it a prospective choice for temporary biomedical systems. PLA's primary monomeric building block exists in L-, D-, or both L/D-lactide forms, influencing the polymer's biodegradability and mechanical properties [13–15]. The primary mechanism of PLA degradation within the body is the hydrolysis of the ester-bond backbone, catalyzed by newly formed carboxylic groups at the end of cleaved PLA chains [16,17]. However, PLA's inherent hydrophobic properties and resistance to hydrolysis result in a slow degradation rate of about two to five years in the crystalline phase hydrolysis [18]. Consequently, PLA may pose complications in tissues and prove unsuitable for use as medical appliances due to its extended degradation period, as observed in applications like surgical suture threads [5]. Blending PLA with natural-based composites or plasticizers stands out as an efficient method to address PLA's inherent disadvantages and broaden its applications [19,20].

Studies [21–24] have successfully demonstrated the positive impact of starch incorporation into PLA composites, enhancing both mechanical and biocompatibility performances for medical applications. However, the utilization of sago starch as a natural-based polymer in PLA implants presents a promising yet limited understanding [25–27]. Recognized for its ability to improve biodegradability, non-toxicity and its consideration as a renewable resource, sago starch encounters challenges in achieving homogeneity, often leading to agglomeration and poor bonding with other materials due to its hydrophilic characteristics [28,29]. To address these challenges, additional polymers such as polyethylene glycol (PEG) are introduced to enhance cohesion among the phase materials. In PLA-based implants, PEG enhances hydrophilicity, surface wettability, elongation percentage and impact strength through copolymerization with PLA [30,31]. However, literature on PLA-based performance in combination with both sago starch and PEG as the plasticizer material remains limited [27].

The addition of starch and PEG can decrease mechanical strength, necessitating careful observation and formulation of the mixing proportions to ensure sufficient strength in PLA products. Adding PEG to the PLA/starch mixture at an 80:20 ratio, based on previous research [32], aims to achieve a balance of strength and stiffness. Exceeding 20% starch addition significantly reduces tensile strength and elongation at the break of PLA. The study explores two variations of PEG addition: 10% and 20% by weight of the PLA/starch mixture, revealing that 10% PEG is more effective in increasing break elongation compared to 20% PEG. Previous findings indicated that adding sago starch up to 20% w/w maintained tensile strength at over 60% of pure PLA, while concentrations beyond that significantly reduced strength to below 36% of pure PLA [27]. PEG increased tensile and bending elongations at break and flexural strength compared to sago starch/PLA blends but reduced tensile strength and elastic modulus, obtained after injection molding at 180 °C. Thermochemical manipulation during the injection molding process, particularly with orientation control systems (SCORIM), can enhance PLA's mechanical properties. SCORIM has been successfully applied to starch-PLA mixture materials for medical applications, as reported in previous study [27]. However, the optimal temperature and polymeric mate-

rial compositions for achieving the desired properties in PLA-based miniplates implants remain unclear.

In short, previous studies have extensively characterized PLA blends for diverse biomedical applications [21,22]. Additionally, a comprehensive examination of a sago starch/PLA/PEG compound, fabricated into miniplate samples with a focus on physico-chemical and mechanical properties, has been reported in the previous paper [27]. However, there is a notable gap in the literature concerning the impact of the manufacturing process when producing PLA in combination with the starch and the plasticizer. Therefore, it is hypothesized that by understanding the balance of injection molding parameter and the mixture composition, the functionality of the PLA-based miniplate implant could be improved. This research aims to assess the effects of variations in injection molding temperatures and sago/PLA/PEG weight compositions to identify the optimal combination for enhancing the mechanical properties and biodegradation behavior of the miniplates. The reported mechanical properties involve the results of tensile and bending tests, revealing information about the strength, elastic modulus and elongation at break of the miniplates. The study also observes the biodegradation performance, aiming to determine if the miniplates exhibit faster degradation compared to the existing result within the observed time period.

2. Material and Methodology

2.1. Materials

The PLA material supplied (Zhuhai Sunlu Industrial Co., Ltd., Zhuhai, China) has a melting point of 155 °C and a molecular weight of 160,000 g/mol. *Metroxylon sago*, known as sago starch (PT ANJAP, South Sorong, Indonesia) contains 27% amylose. PEG 4000 (Merck, Darmstadt, Germany) has a density of 1.2 g/cm^3 and a molecular weight of 4000 g/mol. Methylene chloride (MC) and phosphate-buffered saline (PBS) with pH of 7.3 (Sigma-Aldrich, Darmstadt, Germany) were used for the biodegradability test on miniplate samples.

2.2. Miniplate Samples Preparation

Miniplate samples were prepared using mixed compositions of sago starch, PLA and PEG materials, as detailed in Table 1. The miniplate manufacturing process was conducted using an injection molding machine, specifically the ELITE E-80B (Elite Industrial Holding, Hong Kong, China). The molds utilized in miniplate production were constructed from the main material as per standard DIN 1.2311 for core cavity components. The overall dimensions of the molds were 300 mm × 300 mm × 189 mm, with core cavity dimensions measuring 200 mm × 300 mm × 50 mm.

Table 1. Composition of miniplate samples of sago starch, PLA and PEG blend formulations.

Samples	Chemical Compounds	Weight Fraction of Sago Starch	Weight Fraction of PLA	Weight Fraction of PEG
SPLA20P0	Sago starch/PLA	20	80	0
SPLA0P10	Sago starch/PLA/PEG	0	90	10
SPLA20P10	Sago starch/PLA/PEG	20	70	10
SPLA20P20	Sago starch/PLA/PEG	20	60	20

This study utilized four injection temperature variations, i.e., 150, 160, 170 and 180 °C, on the production of the miniplates. The mold was designed to produce a six-hole miniplate, measuring 1.2 mm in thickness, 6.1 mm in width and 34.0 mm in length [27]. The miniplate manufacturing process involves subjecting the material to an injection pressure of 650 bar, a holding pressure of 500 bar and a water-cooling duration of 24 s.

To ensure optimal performance of the injection machine, the injection stage follows mold installation and initial process trials using pure PLA material. The molding operation initiates at an injection temperature of 150 °C, gradually increasing it until reaches the desired higher temperature. The miniplate samples ready for testing are depicted in Figure 1.

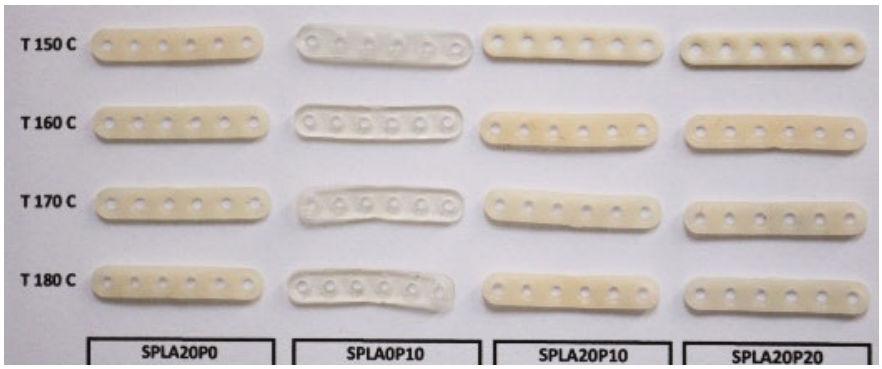

Figure 1. Injection molding miniplate products; miniplate products with variations of PLA/starch mixtures/PEG plasticizer.

2.3. Mechanical Properties Testing

Before conducting mechanical testing, five miniplates were prepared for each sample group. The testing utilized an MCT-2150 universal testing machine (UTM) (A&D Company, Tokyo, Japan), with a maximum force capacity of 500 N and a crosshead speed set at 10 mm/min. The tensile test, in accordance with ASTM D638 standard [33], was employed to determine the tensile strength (TS), Young's modulus (E) and elongation at break (EB). Simultaneously, the bending test, following the ASTM D790 standard [34], was performed to assess the flexural strength, flexural modulus and elongation at break.

2.4. Biodegradation Test

The biodegradation test for the miniplates was conducted in accordance with ISO 10993-5 (E) [35], Part 5 about the biological evaluation of medical devices tests for in vitro cytotoxicity [27]. Miniplate samples were immersed in a falcon tube containing 20 mL of phosphate-buffered saline (PBS) at pH 7.3 ± 0.2 and securely sealed. These samples were then stored in a thermostatic bath maintained at a constant temperature of 37 ± 1 °C for 7, 14, 21 and 28 days. The tests were repeated three times for each variable.

At each designated time point, the pH of the PBS solution was verified, and the samples were withdrawn from the solution and dried at 90 °C for 30 min until a constant weight was achieved. The miniplate loss was calculated using the formula in Equation (1):

$$W_{loss}(\%) = \frac{m_d}{m_o} \times 100\% \quad (1)$$

where $W_{loss}(\%)$ represents the average degradation rate, m_o is the initial weight and m_d is the final weight. Additionally, the result of the degradation mass was presented as the remaining weight, calculated as Equation (2):

$$Remaining\ weight(\%) = 100\% - W_{loss}(\%) \quad (2)$$

2.5. Scanning Electron Microscope (SEM)

The microstructure of the miniplate was examined using a scanning electron microscope (SEM) (FEI Quanta 650, Thermo Fisher Scientific, Waltham, MA, USA) with an acceleration voltage of 7.5 kV. Specimens were prepared under cryogenic conditions using liquid nitrogen and coated with a layer of gold before investigating the surface. The magnification was set to 1500× magnification to analyze the incorporation of sago starch into the

blend of PLA and PEG, only at one chosen injection temperature specimens group based on the result of the biodegradation test.

2.6. Fourier Transform Infra Red (FT-IR) Spectroscopy

The FT-IR spectrum was obtained using the Nicolet™ iS50 Fourier Transform Infrared (FT-IR) spectrometer (Thermo Fisher Scientific, Waltham, MA, USA), with a frequency range of 15–27,000 cm^{-1}, operated using OMNIC Series software version 8.2 (Thermo Fisher Scientific, Waltham, MA, USA). Sample preparation involved cutting cross-sections with a thickness of 1 mm, followed by characterization in accordance with the method employed previously [36]. The measurements were performed at a resolution of 4 cm^{-1} in the wavelength range of 400–4000 cm^{-1}, with an average of 20 scans for each sample. The obtained spectral wavenumbers were compared with literature values to identify functional groups present in the samples with different compositions at only one chosen injection temperature for the specimen's group.

2.7. X-ray Diffraction (XRD)

Characterization with XRD was conducted to determine the primary features of the miniplate, specifically particle size and crystallinity degree. For XRD characterization, a 400 mg sample of the miniplate was taken and placed on a glass slide with the aid of an adhesive. The sample was characterized using a XRD Panalytical Empyrean (Malvern Panalytical, Malvern, UK) with a Cu anode source, and analysis was performed using HighScore Plus software version 3.0e. The applied voltage was 40 kV, and the current was set at 30 mA. The 2θ angle ranged from 10° to 80° with a scanning rate of 0.0263°/step.

The crystallinity degree represents the quantity of crystalline content in a material by comparing the area under the crystalline curve to the total area under the amorphous and crystalline (X_c) was calculated using Equation (3) [27].

$$X_{c(\%)} = \frac{Area\ of\ cristalline\ peaks}{Area\ of\ all\ peaks\ (crystalline\ +\ amorphous)} \times 100\% \quad (3)$$

2.8. Statistical Analysis

The results are displayed as averages with error bars representing the standard deviation (SD). Statistical analysis was conducted using one-way analysis of variance (ANOVA). The tested samples (n = 5) were grouped based on sample weight composition and injection molding temperature for comparison. ANOVA was employed to determine the significance of material compositions and injection temperature effects on the mechanical properties obtained during tensile and bending tests of the miniplate samples. A significance level of α = 0.05 was utilized and the p-value was compared in the mentioned comparisons. Results with a p-value less than 0.05 were considered significantly different and indicated by an asterisk (*) and (**o**) for injection temperature and material compositions effects, respectively.

3. Results

3.1. Tensile Test

Figure 2 details the mechanical properties of miniplates measured through tensile testing, organized by groups of injection molding temperature variations and material weight compositions. It provides a statistical analysis of the mechanical properties obtained from tensile testing of miniplates, including ultimate stress, elastic modulus and break elongation. The categorization is based on groups of injection molding temperature variations and material weight compositions.

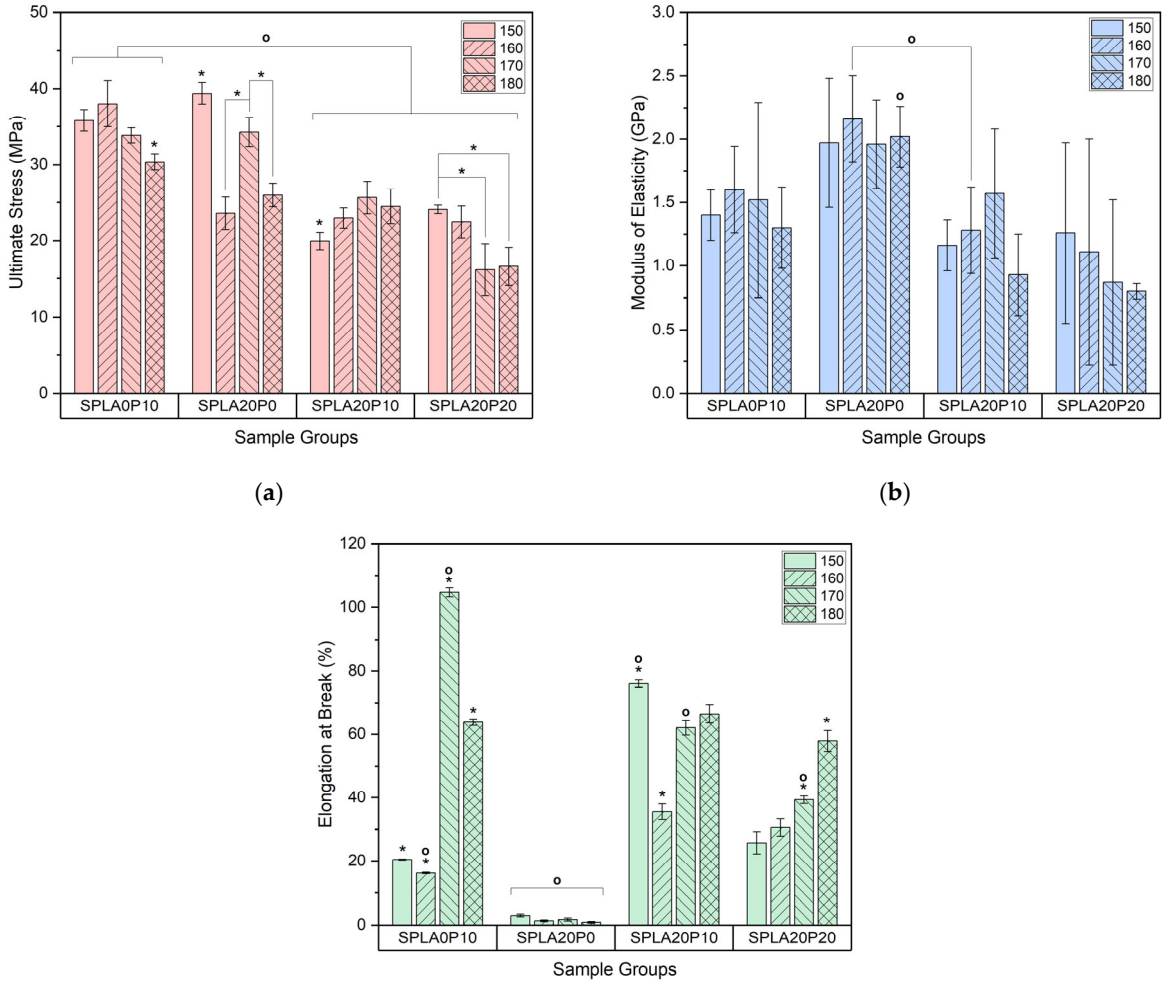

Figure 2. Mechanical properties, including (**a**) ultimate stress, (**b**) modulus of elasticity and (**c**) elongation at break of miniplates obtained from tensile testing, categorized by groups of injection molding temperature variations and material weight compositions ($p < 0.05$; $n = 5$; annotations (**º**) and (*) for material compositions and injection temperature effects, respectively).

Figure 2a depicts that sample groups blending both sago starch and PEG in PLA material (SPLA20P10 and SPLA20P20) with varied injection temperatures generally exhibited lower ultimate stresses compared to the remaining sample groups, particularly distinct from the sample group without sago starch (SPLA0P10, ranging between 30.34 ± 1.03 MPa to 38.00 ± 3.02 Mpa). Most sample groups displayed a trend of significantly reducing ultimate stress with increasing injection mold temperature, such as SPLA0P10 from 38.00 ± 3.02 Mpa at 160 °C to the lowest of 30.34 ± 1.03 Mpa at 180 °C, SPLA20P0 from 39.37 ± 1.40 at 150 °C to 25.96 ± 1.57 Mpa at 180 °C and SPLA20P20 from the highest of 24.05 ± 0.57 Mpa at 150 °C to 16.58 ± 2.5 Mpa at 180 °C. The SPLA20P10 sample group, however, showed an increasing trend in ultimate stress over higher temperatures, although it was only significant below 160 °C of 22.93 ± 1.34 Mpa.

Figure 2b depicts that sample groups with PEG had lower elastic modulus, with the lowest of 0.8 ± 0.06 Gpa at 180 °C in SPLA20P20, compared to the sample groups without PEG blend (SPLA20P0, ranging between 1.96 ± 0.35 Gpa to 2.16 ± 0.34 Gpa). Nevertheless, the overall trends were not statistically different, except for the comparison between SPLA20P0 and SPLA20P10, respectively, resulting 2.16 ± 0.34 GPa and 1.28 ± 0.34 GPa, at the 160 °C temperature. Additionally, SPLA20P0 samples at 180 °C showed a significant increase of 2.02 ± 0.24 GPa compared to the remaining sample groups

at similar temperature settings, as the highest of 1.3 ± 0.32 GPa in the SPLA0P10 group. No significant differences were observed when comparing molding temperature variations within each sample group.

Figure 2c presents the break elongation results, indicating that sample groups without PEG (SPLA20P0, ranging between 0.87 ± 0.30% to 2.99 ± 0.46%) had the lowest values compared to the remaining groups at each molding temperature. Sample groups with PEG blend showed incremental break elongations with increasing injection mold temperatures. Statistical significance was observed in SPLA010 from temperatures of 150 and 160 °C (20.38 ± 0.20% and 16.17 ± 0.24%, respectively) to 170 and 180 °C (104.64 ± 1.41% and 63.83 ± 1.01%, respectively), SPLA20P10 from 35.50 ± 2.46% at 160 °C to higher temperatures and SPLA20P20 with a gradual trend from 25.73 ± 3.53% at 150 °C reaching to 57.85 ± 3.38% at 180 °C. Interestingly, SPLA20P20 samples exhibited lower elongation at break results compared to sample groups containing 10% PEG, such as SPLA0P10 and SPLA20P10.

The obtained stress–strain curves from one of the tensile testing repetitions of miniplate samples are also illustrated in Figure 3.

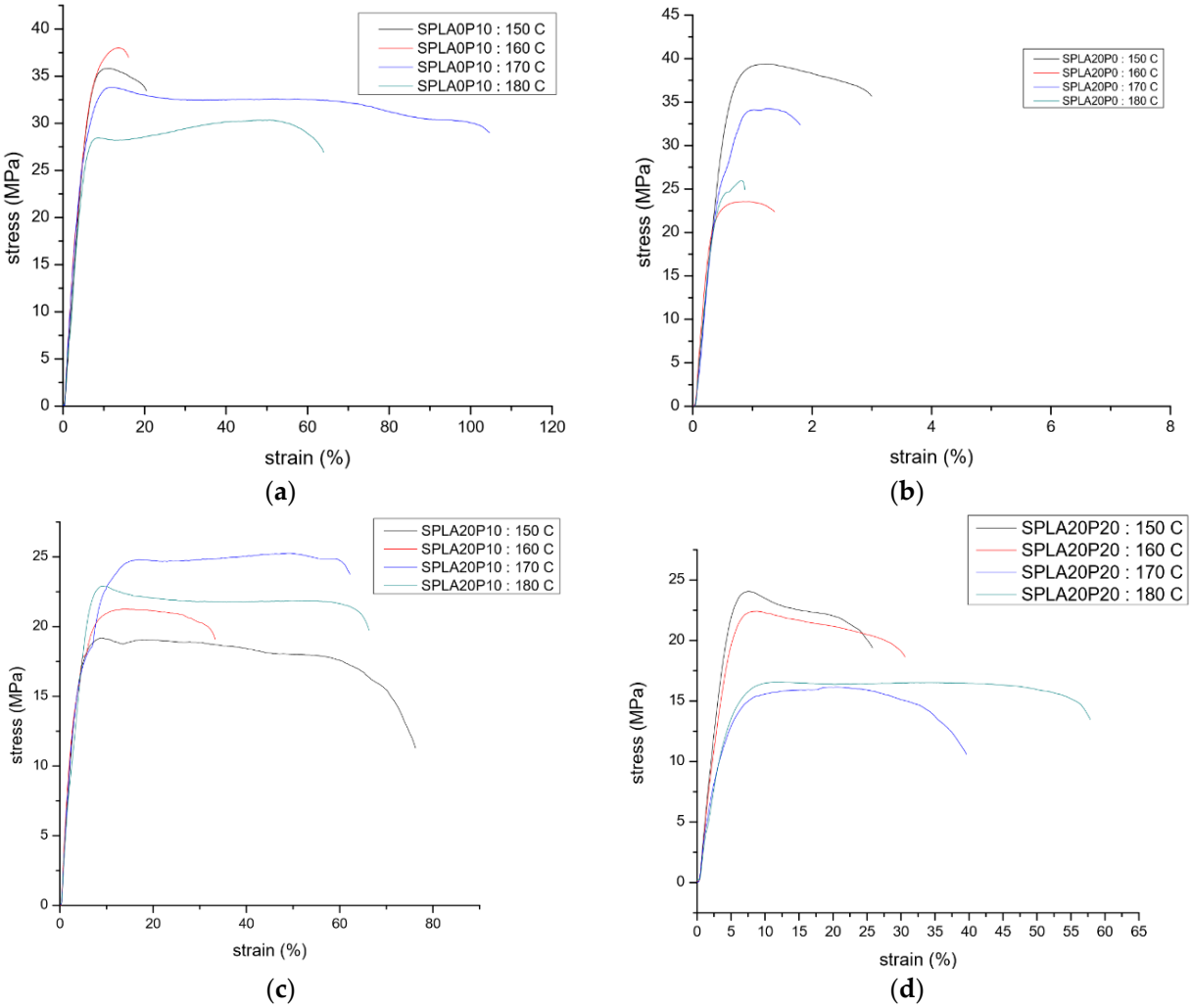

Figure 3. Stress–strain curves of miniplate samples with varied injection molding temperatures resulting from tensile testing, grouped by sample compositions: (**a**) SPLA0P10, (**b**) SPLA20P0, (**c**) SPLA20P10 and (**d**) SPLA20P20.

3.2. Bending Test

Figure 4 provides an overview of the mechanical properties of miniplates measured through bending testing, organized by groups of injection molding temperature variations and material weight compositions. It presents the statistical analysis of miniplate properties obtained through bending testing, categorized by groups of injection molding temperature variations and material weight compositions.

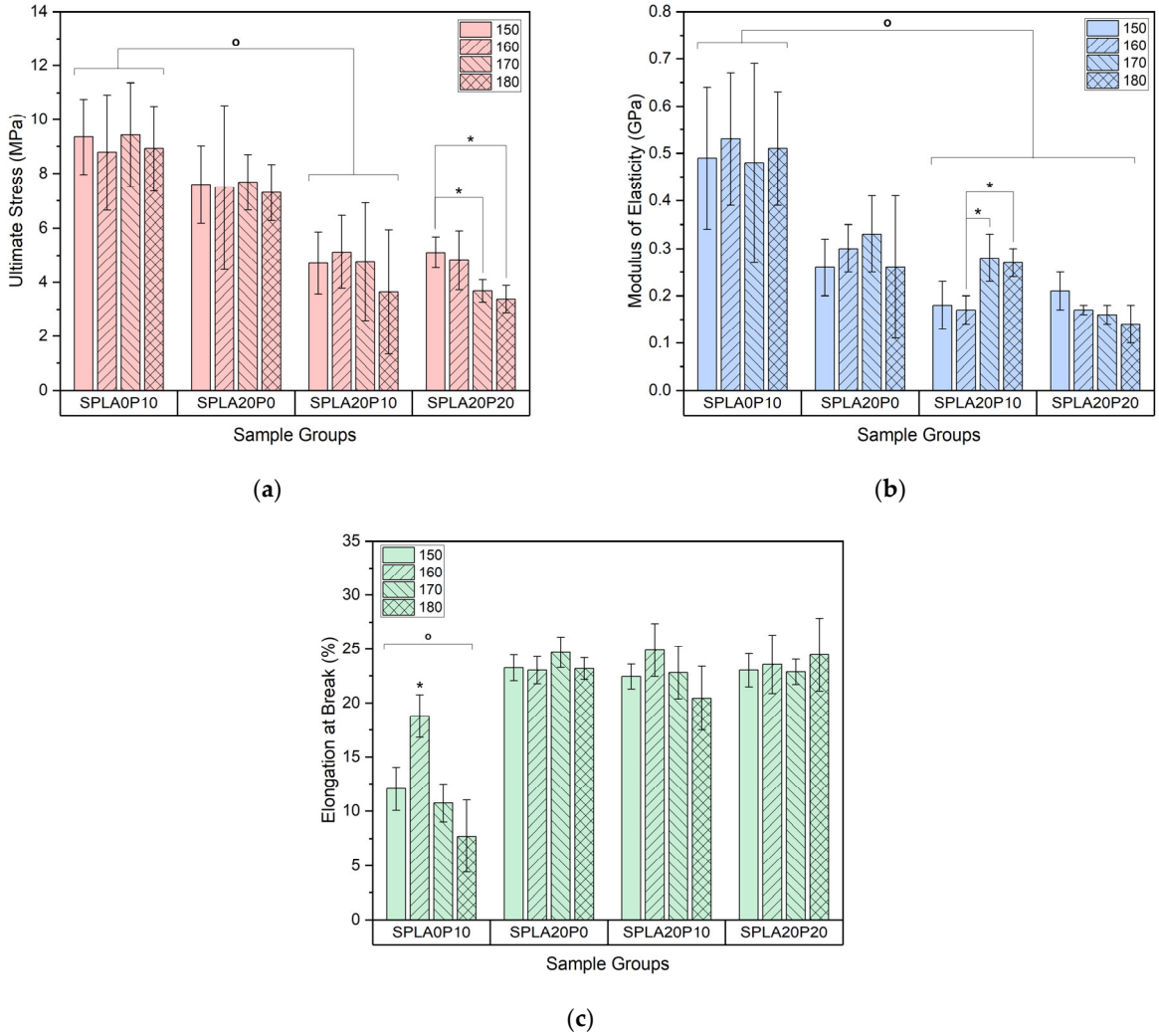

Figure 4. Mechanical bending properties, including (**a**) ultimate stress, (**b**) bending modulus of elasticity and (**c**) elongation at break of miniplates obtained from bending testing, categorized by groups of injection molding temperature variations and material weight compositions ($p < 0.05$; $n = 5$; annotations (**º**) and (*) for material compositions and injection temperature effects, respectively).

In Figure 4a, the SPLA20P10 and SPLA20P20 sample groups demonstrated lower ultimate stresses for all injection mold temperatures compared to the remaining two groups. Notably, a significant difference was observed when comparing SPLA20P10 and SPLA0P10 sample groups. No statistical differences were found when comparing different temperature settings within each sample group, except for a significant reduction trend over the increasing injection temperature in the SPLA20P20 sample group, ranging from 5.109 ± 0.57 MPa at 150 °C to 3.38 ± 0.50 MPa at 180 °C.

Figure 4b indicates that sample groups containing sago starch exhibited lower elastic modulus compared to the SPLA0P10 sample group. Statistical evidence supports this observation in the SPLA20P10 and SPLA20P20 samples. The modulus of elasticity behavior generally remained unclear, showing no significant difference with respect to the effect of

injection molding temperature within each sample group. However, in the SPLA20P10 sample group, there was a clear trend of steady increment over the increasing temperature, specifically from 0.17 ± 0.03 GPa at 160 °C to above 0.27 ± 0.03 GPa at higher temperature settings.

Figure 4c reveals that only the non-sago sample group (SPLA0P10) had significantly lower break elongation results across all injection mold temperatures, with the highest at 18.78 ± 1.98% at 160 °C. The remaining temperatures exhibited break elongation ranging from 7.70 ± 3.30% to 12.05 ± 1.99% in that group. The remaining sample groups with sago blend consistently showed a range of break elongation between 20.44 ± 2.95% to 24.9 ± 2.46% without any substantial differences.

The obtained stress–strain curves of miniplate samples from the bending test process are illustrated in Figure 5, providing a visual representation from one of the tensile testing repetitions of miniplate samples material behavior under bending stress.

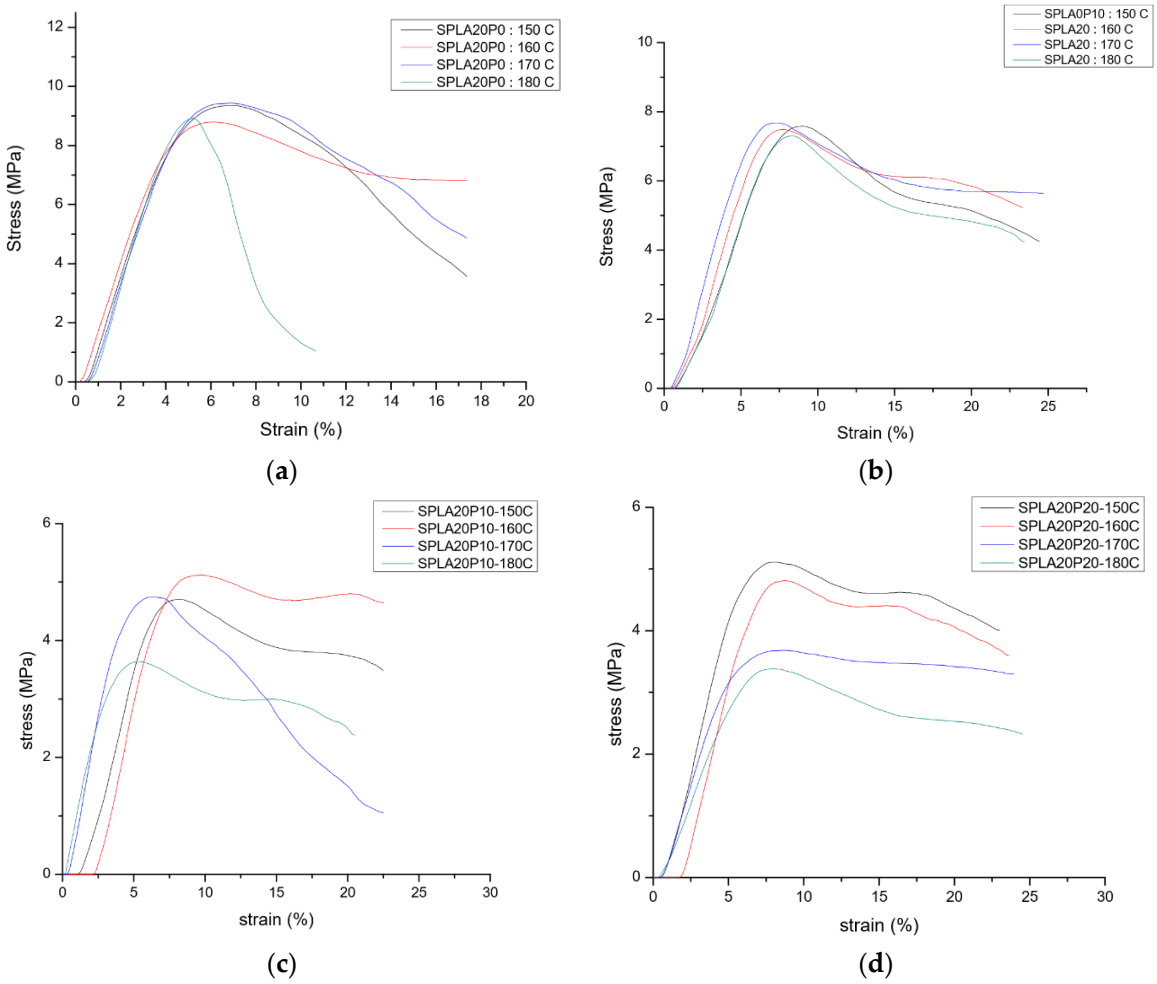

Figure 5. Stress–strain curves of miniplate samples with varied injection molding temperatures obtained from bending testing, grouped by sample compositions: (**a**) SPLA0P10, (**b**) SPLA20P0, (**c**) SPLA20P10 and (**d**) SPLA20P20.

3.3. Biodegradation Test

Figure 6 presents the percentage of mass loss over immersion days from the biodegradation rate test of miniplate samples with varied injection molding temperatures, grouped by sample compositions. In Figure 6a, the degradation rate of miniplates with the addition of 10% PEG plasticizer to the PLA matrix without sago starch blend (SPLA0P10) is depicted. The mass loss percentage at 7 days after treatment was 1.04% at 150 °C, 1.02% at 160 °C, 1.84% at 170 °C and 2.54% at 180 °C. Degradation slowed down on the 14th day, with no

degradation observed at 150 °C and 160 °C. At 170 °C, there was a mass loss of 0.21% and at 180 °C, the highest mass loss percentage was recorded at 0.62%. By the 21st day, mass loss at 150 °C increased to 2.67%, at 160 °C there was a mass loss of 0.82%, at 170 °C it was 0.42% and at 180 °C of 0.83%.

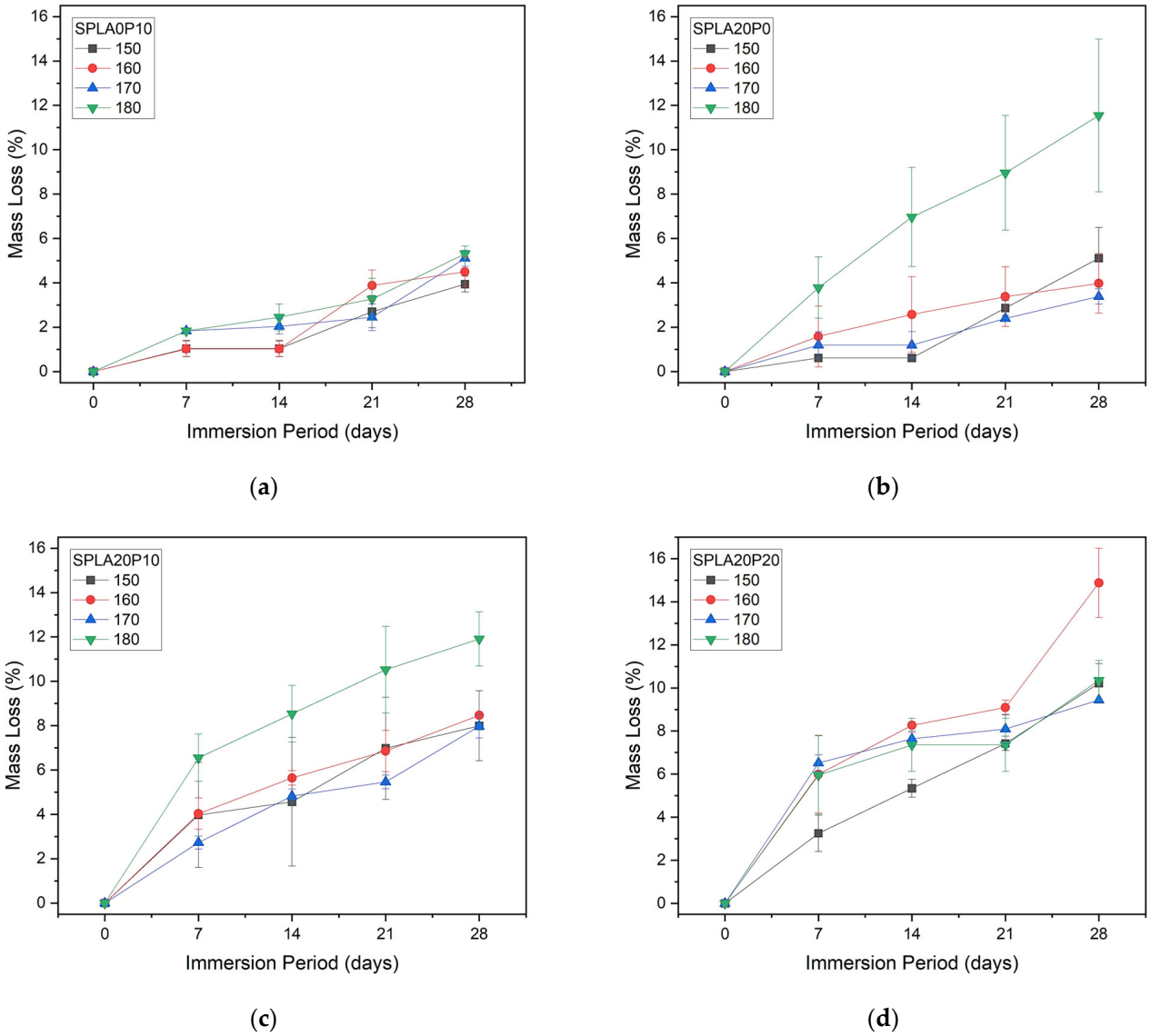

Figure 6. Average mass loss percentage over immersion days during biodegradation rate test of miniplate samples with varied injection molding temperatures grouped by sample compositions: (**a**) SPLA0P10, (**b**) SPLA20P0, (**c**) SPLA20P10 and (**d**) SPLA20P20 (n = 3).

Figure 6b illustrates how changes in injection temperature impacted the mass loss percentage of SPLA20P0 miniplates derived from PLA/starch mixtures. The mass loss percentage after 7 days of treatment was 0.61% at 150 °C, 1.58% at 160 °C, 1.2% at 170 °C and 3.78% at 180 °C. The highest mass loss percentage was observed at 180 °C, while the lowest was at 150 °C. On the 14th day, degradation slowed down, with no degradation observed at 150 °C and 170 °C. At 160 °C, there was a mass loss of 1.01%; at 180 °C, the highest mass loss percentage was recorded at 3.35%. By the 21st day, mass loss at 150 °C increased to 2.26%, at 160 °C there was a mass loss of 0.82%, at 170 °C it was 1.21% and at 180 °C it reached 2.17%. The mass loss percentage of miniplates SPLA0P10 was slower than that of SPLA20P0, suggesting that the presence of starch impacted the mass loss percentage.

Figure 6c illustrates the mass loss percentage of miniplates with the addition of 10% PEG plasticizer to the PLA/sago starch mixture (SPLA20P10). Similar to SPLA20P0 and SPLA0P10, changes in injection temperature affected the miniplate's mass loss percentage. The mass loss percentage at 180 °C was higher compared to lower temperatures, while at 150 °C and 160 °C, it remained uniform up to 7 days of treatment. The mass loss percentage at 7 days after treatment was 3.97% at 150 °C, 4.03% at 160 °C, 2.73% at 170 °C and 6.55% at 180 °C. On the 14th day, mass loss slowed down, with mass loss of 0.63% at 150 °C, 1.67% at 160 °C, 2.16% at 170 °C and 2.12% at 180 °C. By the 21st day, mass loss at 150 °C increased to 2.52%, at 160 °C there was a mass loss of 1.28%, at 170 °C it was 0.66% and at 180 °C reached 2.18%. The mass loss percentage increased with the increase in injection temperature.

Figure 6d illustrates the effect of adding 20% PEG plasticizer to the PLA/sago starch mixture on the mass loss percentage (SPLA20P20). Changes in injection temperature did not seem to affect the mass loss percentage, although at 150 °C, it had the lowest mass loss percentage compared to other temperatures. The mass loss percentage at 7 days after treatment was 3.25% at 150 °C, 5.99% at 160 °C, 5.25% at 170 °C and 5.96% at 180 °C. On the 14th day, mass loss slowed down, with mass loss of 2.15% at 150 °C, 2.39% at 160 °C, 1.2% at 170 °C and 1.47% at 180 °C. By the 21st day, mass loss at 150 °C was 2.2%, at 160 °C it was 0.9%, at 170 °C it was 0.49% while at 180 °C there was no mass loss. Based on the graph, it can be concluded that the injection temperature affected the mass loss percentage of the miniplate with the addition of 20% PEG to the PLA matrix/sago starch. The mass loss percentage at 160 °C, 170 °C and 180 °C increased uniformly at 7 days after treatment, while at 150 °C, the mass loss percentage was slower. The mass loss percentage at 150 °C had a difference of 1.1% in the 7, 14 and 21-day immersions. At an injection temperature of 180 °C, there was no decrease in sample weight between 7–14 days.

3.4. SEM Results

Figure 7 shows the micrograph profiles of miniplates after undergoing degradation testing for 28 days of all samples with injection temperature of 180 °C. Figure 7a illustrates the surface condition of a miniplate with PLA/PEG 10% material, revealing surface roughness after degradation. The rough surface profile, indicated by small spots, represents starch particles that emerge during degradation. The circular profile with a brighter color on the surface indicates the presence of starch particles that are not perfectly dispersed in the PLA matrix during the injection molding process.

Figure 7b displays the micrograph profile of the miniplate surface with a 20% sago starch/PLA mixture, providing information about the presence of a relatively large longitudinal crack profile with small perpendicular crack branches around the main crack after 28 days of degradation. The cracks indicate the weak interface bond between starch and PLA matrix due to differences in hydrophilicity.

After a degradation period of 28 days, it is observed that the addition of 10% PEG to the PLA/sago starch mixture does not lead to the emergence of surface crack profiles, indicating that the plasticizing function of PEG is effective in improving the interfacial bond between starch and PLA matrix. The previously formed interface layer around imperfectly dispersed starch particles disappear, forming a clear boundary on the outer side of the starch particles, as in Figure 7c. This suggests that the PEG interface layer will disperse into the PBS solution and degrade more rapidly during degradation.

A clearer profile is observed in the micrograph of miniplates with the addition of 20% PEG to the PLA/sago starch mixture as seen in Figure 7d. The presence of large crack profiles in the image indicates increased porosity due to the higher concentration of PEG dispersed in the PLA/sago starch mixture. The PEG interface layer on starch molecules will degrade faster, carrying along bound starch molecules, while the cracks indicate uneven distribution of plasticizer concentration, causing faster release of the PLA/sago starch interfacial bond compared to lower PEG concentrations. From the micrograph profiles, it can be concluded that the addition of 20% PEG will increase the porosity of miniplates during degradation compared to the addition of 10% PEG to the PLA/sago starch mixture.

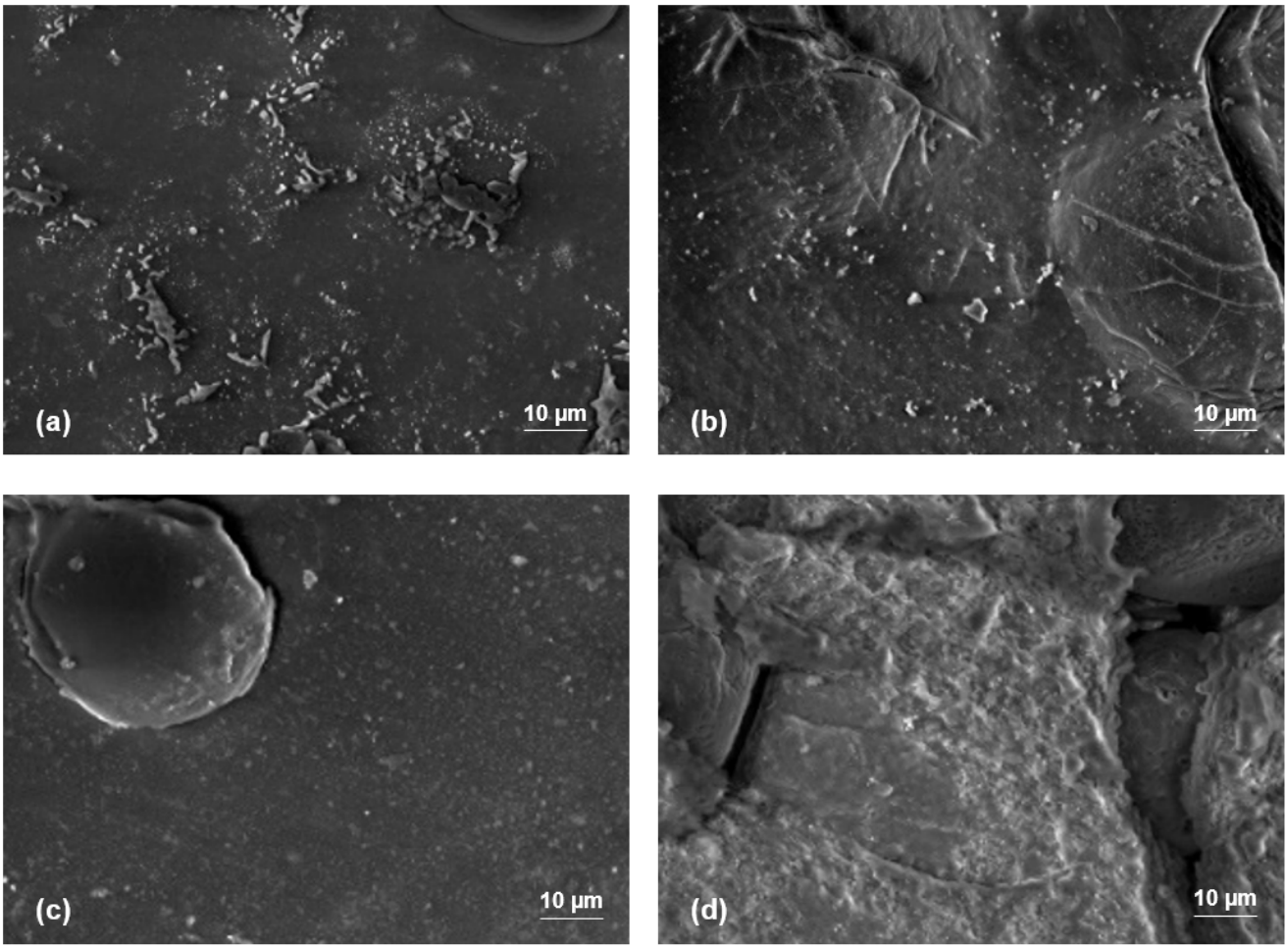

Figure 7. SEM images of different miniplate specimens comparing compositions: (**a**) SPLA0P10, (**b**) SPLA20P0, (**c**) SPLA20P10 and (**d**) SPLA20P20 with injection molding temperature of 180 °C.

3.5. FT-IR Analysis

The interaction between polymers can be observed through the results of infrared spectroscopy (IR), as shown in Figure 8. It can be observed that the miniplate with pure PLA material (SPLA0) has several wave peaks at 1042 cm^{-1}, 1079 cm^{-1}, 1127 cm^{-1}, 1180 cm^{-1}, 1451 cm^{-1} and 1745 cm^{-1}. Peaks at 1042 cm^{-1}, 1079 cm^{-1}, 1127 cm^{-1}, and 1180 cm^{-1} indicate the presence of -C-O bonds, while 1451 cm^{-1} signifies CH_3 bonding, and 1745 cm^{-1} indicates the presence of the -C=O group, referred to in the previous study [27]. The addition of 10% PEG into the PLA matrix (SPLA0P10) shows three peaks indicating the absorption of -CH_2- stretching vibrations at wave numbers 2882, 2944 and 2994 cm^{-1}, as confirmed Li et al. [37]. The increased intensity at 1382 and 1452 cm^{-1} represents the deformation of C-H peaks, indicating the presence of -CH_2 chains from PEG. Characteristics of C=O stretching and C-O stretching from ester groups in PLA and PLA/PEG 10% are shown at wave numbers 1180 and 1747 cm^{-1}. The influence of adding PEG plasticizer with different concentrations (10% and 20%) to the PLA/starch blend can be observed from the wave numbers 2888 and 2994 cm^{-1}, as well as 1747 cm^{-1}, where the peak ratio increases in C-O and C=O in the 10% PEG addition (SPLA20P10) compared to the 20% PEG addition (SPLA20P20). This suggests that a portion of the O-H groups from PEG is likely to bond with the C=O groups in PLA [37].

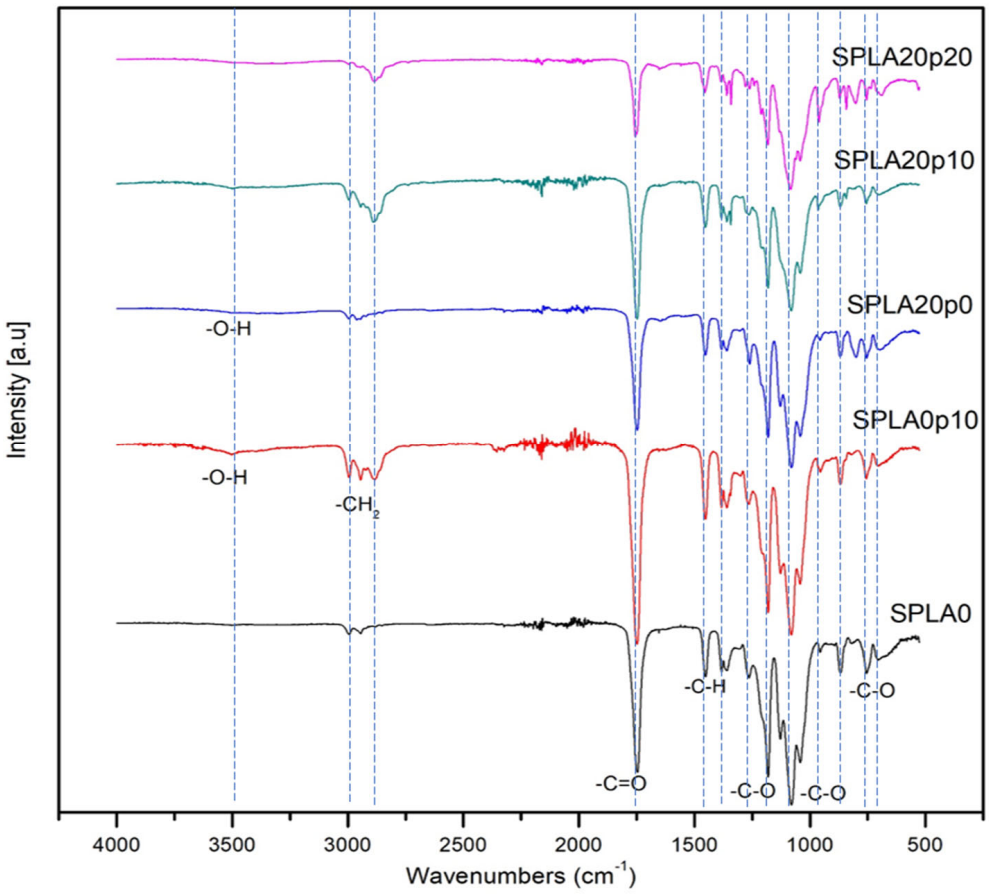

Figure 8. Fourier transform-infrared (FT-IR) spectra for pure PLA compared to various sample compositions of SPLA0P10, SPLA20P0, SPLA20P10 and SPLA20P20 with injection molding temperature of 180 °C.

The interaction between sago starch and PLA can be observed in the wave number range of 3000–3500 cm^{-1}, where there is no increase in waves in pure PLA (SPLA0) but an increase is observed in PLA/sago starch (SPLA20P0). This indicates the presence of -OH bonds in PLA/sago starch [38,39]. When compared to the addition of PEG to PLA, the wave peaks become higher in that wave number range, indicating the influence of PEG plasticizer on both PLA and the PLA/sago starch blend [38]. The occurrence of interactions, such as hydrogen or dipolar interactions, between two polymers will manifest as changes in the observed IR spectrum. FT-IR testing on miniplate products from injection molding aimed to investigate conformational changes in the PLA/sago starch/PEG composite. Previous research by [36] explained that starch gelatinization and retrogradation are sensitive to changes in polymer conformation and molecular-level changes. The C-C and C-O stretching regions (800–1300 cm^{-1}) are highly sensitive to retrogradation processes, where retrogradation kinetics involve structural changes at the molecular level by measuring the ratio between selected peaks [40].

3.6. XRD Analysis

Figure 9 illustrates the X-ray patterns on miniplates derived from pure PLA, PLA with the addition of 10% PEG, PLA/starch 20%, PLA/starch/PEG 10% and PLA/starch/PEG 20%. Characteristic starch reflections at 2θ are seen at 15.2°, 17.3° and 23.1°, while PLA reflections are at 16.7° and 19.0°, corresponding to the starch crystallization pattern [41]. PEG reflections are observed at 14.7°, 16.6° and 18.9° [42].

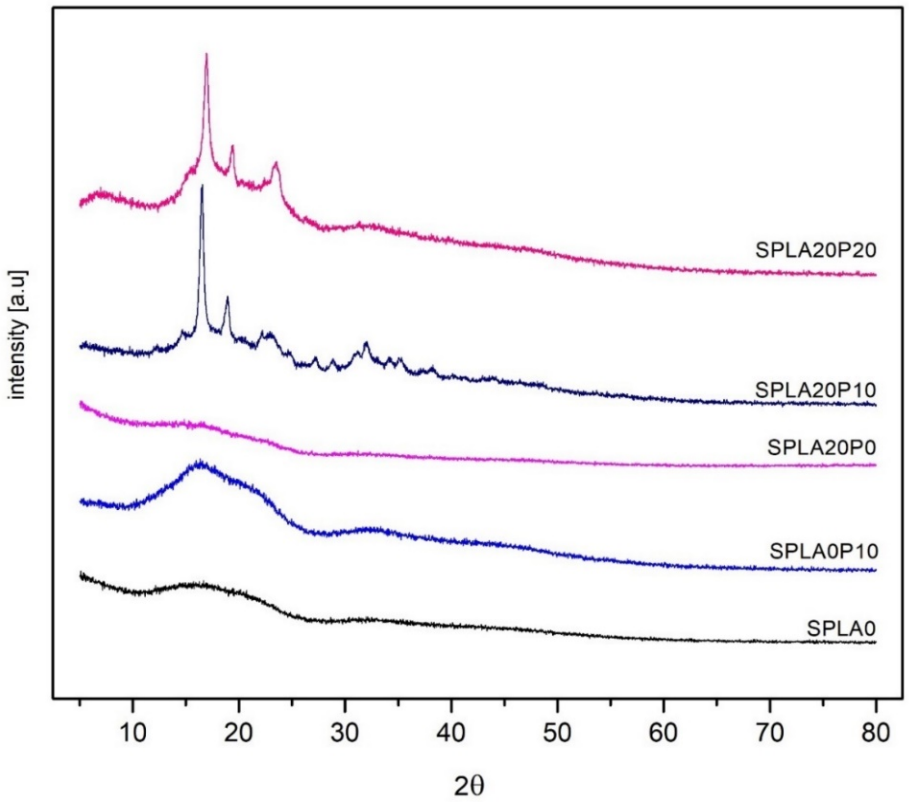

Figure 9. The crystalline phase and molecular interaction of the miniplate specimens with pure PLA compared to various sample compositions of SPLA0P10, SPLA20P0, SPLA20P10 and SPLA20P20 with injection molding temperature of 180 °C.

On miniplates with pure PLA material (SPLA0), amorphous peaks are observed at 2θ around 16.97° and 17.01°, corresponding to crystallographic lattice planes 110 and 200, with weak diffraction peaks at 2θ = 34.6° and 34.7° corresponding to crystallographic lattice plane 21.6, referred to in the previous study [27]. The diffraction peak at 16.97° indicates the amorphous structure of PLA [43]. In miniplates with the addition of 10% PEG to PLA (SPLA0P10), diffraction peaks are observed at 2θ around 18.28° and 18.33°, corresponding to crystallographic lattice plane 203 with a d-spacing value of 0.484 nm, and weak diffraction peaks at 2θ = 32.5° corresponding to crystallographic lattice plane 216. Adding sago starch to the PLA matrix (SPLA20P0) results in diffraction peak patterns at 2θ = 16.35° and 16.39° corresponding to crystallographic lattice planes 110 and 200. In miniplates with the addition of 10% PEG to the PLA matrix (SPLA20P10), diffraction peaks vary at 2θ between 14.74°, 16.48° (highest peak 2386), 17.8°, 18.9°, up to 44.01° corresponding to crystallographic lattice planes 110, 200, 203, 015 and 216. The same diffraction peak pattern occurs with the addition of 20% PEG to the PLA matrix (SPLA20P20), but there is a shift in the highest peak with 2θ = 16.91° (highest peak 1879), resulting in a peak shift of 0.43° from 16.48° to 16.91°. This indicates that an increase in PEG concentration in the PLA/sago starch blend will shift the crystallinity peaks of the composite. It is evident that the addition of PEG plasticizer to the PLA/sago blend will increase the crystallinity (X_c) of PLA, with the crystallinity of SPLA20P10 (45.26%) higher than SPLA20P20 (40.63%). This proves that, in general, the addition of PEG plasticizer to the PLA/sago blend will increase crystallinity, and the addition of 10% PEG is more effective than the addition of 20% PEG.

4. Discussions

This study successfully demonstrated the tunability of injection molding parameters for manufacturing miniplate implants, assessing their mechanical and biodegradation performances with varied compositions of PLA, sago starch and PEG at different injection

temperatures (150 °C, 160 °C, 170 °C and 180 °C). Optimal conditions for miniplate fabrication were identified at 170 °C for PLA/sago starch with 10% PEG, yielding favorable mechanical properties and a degradation rate of 7.97% over 28 days. For PLA/starch with 20% PEG, optimal conditions were at 150 °C, resulting in specific mechanical properties and a degradation rate of 10.22%.

Mechanical assessments revealed that incorporating PEG into pure PLA (SPLA0P10) resulted in relatively high mechanical performance, showing a linear correlation with increasing injection temperature. The optimal composition and injection temperature for mechanical properties were identified as SPLA0P10 at 170 °C and 180 °C, achieving high ultimate stress, elastic modulus and break elongation. These findings were corroborated by bending tests, emphasizing the favorable mechanical aspects of SPLA0P10 at 170 °C. On the other hand, the addition of sago starch to pure PLA material (SPLA20P0) significantly increased ultimate stress, surpassing that of PLA/PEG with no sago (SPLA0P10). However, it also led to a notable decrease in elongation at break across different temperature settings, as observed in both tensile and bending tests. It was suggested that achieving higher mechanical properties for SPLA0P10 required injection molding at higher temperatures (180 °C in this study), while lower temperatures (150 °C in the current study) seemed more effective for SPLA20P0 to achieve high ultimate stress and elastic modulus. Interestingly, the addition of sago starch and PEG together to the PLA, as observed in SPLA20P10 and SPLA20P20, resulted in a general decrease in mechanical performance across the tested temperatures, indicating an antagonistic interaction between sago starch and PEG plasticizer when blended into the PLA-based implant, affecting its mechanical resistance.

Nevertheless, the inclusion of sago starch proved effective in optimizing the biodegradation rate of the PLA miniplate implant, necessitating comprehensive characterization to determine the most optimal compositions and manufacturing parameters when combining the three materials: PLA, sago and PEG plasticizer. A higher biodegradation rate was observed with a larger weight composition of the hydrophilic component, primarily due to the presence of sago starch. In general, the PEG interphase layer enhanced the interface between PLA and sago starch, as confirmed in SEM imaging of the miniplate with a PEG content of 10% by weight (SPLA20P10) in a previous study [27]. An increase in the sago starch content in the PLA blend significantly improved the mass loss rate of the miniplate samples. A comprehensive review on the biodegradation of PLA in medical implants and systems has been conducted by da Silva et al. indicating that the degradation rate of PLA material inside the human body primarily occurs through the hydrolysis of its ester-bond polymeric backbone. This process is commonly dependent on lactide shapes, porosity structure, pH and temperature of the surrounding environments [44–46]. However, PLA's inherent hydrophobic properties and resistance to hydrolysis result in a slow degradation rate in crystalline phase hydrolysis, posing a challenge in tissues and rendering it unsuitable for use as medical appliances due to its extended degradation period [5,18]. Diyana et al. [24] have provided an overview of the physical properties of thermoplastic starch made of natural resources, stating that as a blend component for PLA, starch offers important advantages in terms of cost, mechanical properties and biodegradability. However, the hydrophilic characteristics of starch and the hydrophobic features of PLA cause low miscibility between the two compounds, necessitating good melt-blending techniques and the addition of compatibilizers to ensure successful interaction [47]. Furthermore, PEG content in PLA material was observed to increase biodegradation rate, indicated by the enhancing weight loss over time in the previous studies [48–50]. The high PEG will increase the hydrophilic behavior than the ones with lower content, thus it was easier to dissolve in PBS solution.

These findings suggest that it might be more beneficial in terms of mechanical properties when only one of the materials, either sago starch or PEG, is mixed with pure PLA for the implant at the specified injection temperature. On the other hand, sago starch is required to enhance the biodegradability rate, whereas PEG is needed to increase the homogeneity of the mixture and minor elastic modulus. Injection molding parameters play

a key role in balancing both mechanical and biodegradation performances, with higher injection temperatures generally accelerating the degradation rate and break elongation percentage of the PLA/sago starch/PEG miniplates. Previous findings [27] have shown inadequate interfacial interaction between starch and PLA, evident in the consistent reduction of tensile strength with higher concentrations of sago starch. Another study by Bhiogade et al. [43] indicated that the addition of PEG plasticizers significantly reduces tensile strength and modulus of elasticity. Despite this, PEG remains necessary as it improves the homogeneity interaction between PLA and starch interfaces, acting as a molecular bridge [51]. This is crucial because PLA is hydrophobic, while sago starch is hydrophilic, resulting in expected poor interaction [52,53]. The additional PEG molecular chain acts as an efficient compatibilizer in the PLA/sago starch mixture. Consequently, adding PEG plasticizers to the PLA/starch mixture leads to a reduction in both the modulus of elasticity and tensile strength. This finding is supported by Ferrarezi [38] and Kozlowski [54], who observed that the addition of PEG significantly increased the drawability of the miniplate but decreased the elastic modulus. During the injection molding process, as the PLA matrix deforms under pressure and increased shear forces, the PEG interface effectively forms around the starch particles. As a result, the PEG can impede the formation of fractures, leading to a significant increase in the break elongation of the miniplate. An exception in this study was only observed in SPLA20P10 at 170 °C, showing better performance in elastic modulus and elongation at break, indicating the role of injection temperature in molding the miniplate implant.

Based on the findings of this study, miniplates comprising PLA/sago starch/PEG fall short of meeting the mechanical requirements for bone implants. To enhance the mechanical properties of the miniplates, which possess favorable mechanical properties and degradation capability, can be considered [55,56]. The ability to withstand bending loads is particularly critical for materials used in bone implants, especially in high-risk areas such as the bones of the arms and legs, which are subjected to significant bending loads during various activities. For example, cortical bone exhibits a bending strength ranging from 130–180 MPa, whereas miniplates SPLA20P10 and SPLA20P20 demonstrate strengths below this threshold. Consequently, miniplates composed of PLA/sago starch/PEG are better suited for application in bone tissues that do not necessitate high bending loads, such as skull fractures and craniofacial fractures.

5. Conclusions

This study effectively investigated the optimal parameters of injection molding temperature and plasticizer material to enhance the mechanical and biodegradation performances of PLA-sago starch miniplates implants. Several key findings can be drawn to conclude as follow:

- Optimal conditions for miniplate fabrication were identified at 170 °C for PLA/sago starch with 10% PEG, yielding favorable mechanical properties and a degradation rate of 7.97% over 28 days. For PLA/starch with 20% PEG, optimal conditions were at 150 °C, resulting in specific mechanical properties and a degradation rate of 10.22%.
- An antagonistic interaction between the sago starch and PEG plasticizer was indicated when blended into the PLA-based implant, affecting its mechanical properties.
- However, the role of sago starch concentration in the mixture resulted in an increased biodegradation rate.
- The addition of PEG plasticizer also had an impact on mechanical properties, yet it was attributed to the formation of an interphase layer by the PEG plasticizer, enhancing interaction between PLA and starch interfaces, indicated via SEM images.
- The higher injection molding temperatures were found to generally accelerate the degradation rate and break elongation percentage, which play a key role in balancing both mechanical and biodegradation performances of the PLA/sago starch/PEG miniplates.

The study significantly contributes to enhancing the value of agricultural products, especially sago starch, in the medical field by improving miniplate products biomaterial through advanced fabrication methods.

Author Contributions: Conceptualization, Y.W., S.S. and A.A.; methodology, Y.W. and S.S.; software, M.C.; validation, A.A., S.S. and P.K.; formal analysis, Y.W. and M.T.; investigation, M.T. and M.C.; resources, Y.W., M.C. and A.A.; data curation, Y.W. and M.T.; writing—original draft preparation, Y.W.; writing—review and editing, M.T. and Y.W.; visualization, M.C. and M.T.; supervision, Y.W., P.K. and A.A.; project administration, Y.W.; funding acquisition, Y.W. All authors have read and agreed to the published version of the manuscript.

Funding: This work was supported by the Universitas Indonesia PUTI Grant 2022 NKB-1354/UN2.RST/HKP.05.00/2022.

Data Availability Statement: The data supporting the conclusions of this article will be made available by the authors on request. Further inquiries can be directed to the corresponding author/s.

Conflicts of Interest: The authors declare no conflicts of interest.

References

1. Arya, S.; Bhatt, K.; Bhutia, O.; Roychoudhury, A. Efficacy of bioresorbable plates in the osteosynthesis of linear mandibular fractures. *Natl. J. Maxillofac. Surg.* **2020**, *11*, 98–105. [CrossRef] [PubMed]
2. Chocron, Y.; Azzi, A.J.; Cugno, S. Resorbable Implants for Mandibular Fracture Fixation: A Systematic Review and Meta-Analysis. *Plast. Reconstr. Surg. Glob. Open* **2019**, *7*, e2384. [CrossRef] [PubMed]
3. Kim, D.Y.; Sung, I.Y.; Cho, Y.C.; Park, E.J.; Son, J.H. Bioabsorbable plates versus metal miniplate systems for use in endoscope-assisted open reduction and internal fixation of mandibular subcondylar fractures. *J. Cranio-Maxillofac. Surg.* **2018**, *46*, 413–417. [CrossRef] [PubMed]
4. Nurmi, J.T.; Itälä, A.; Sihvonen, R.; Sillanpää, P.; Kannus, P.; Sievänen, H.; Järvinen, T.L.N. Bioabsorbable Versus Metal Screw in the Fixation of Tibial Tubercle Transfer: A Cadaveric Biomechanical Study. *Orthop. J. Sports Med.* **2017**, *5*, 2325967117714433. [CrossRef] [PubMed]
5. Kanno, T.; Sukegawa, S.; Furuki, Y.; Nariai, Y.; Sekine, J. Overview of innovative advances in bioresorbable plate systems for oral and maxillofacial surgery. *Jpn. Dent. Sci. Rev.* **2018**, *54*, 127–138. [CrossRef] [PubMed]
6. Lasprilla, A.J.; Martinez, G.A.; Lunelli, B.H.; Jardini, A.L.; Filho, R.M. Poly-lactic acid synthesis for application in biomedical devices—A review. *Biotechnol. Adv.* **2012**, *30*, 321–328. [CrossRef] [PubMed]
7. Hur, W.; Park, M.; Lee, J.Y.; Kim, M.H.; Lee, S.H.; Park, C.G.; Kim, S.N.; Min, H.S.; Min, H.J.; Chai, J.H.; et al. Bioabsorbable bone plates enabled with local, sustained delivery of alendronate for bone regeneration. *J. Control. Release* **2016**, *222*, 97–106. [CrossRef]
8. Chapman, S. The radiological dating of injuries. *Arch. Dis. Child.* **1992**, *67*, 1063–1065. [CrossRef]
9. Park, Y.W. Bioabsorbable osteofixation for orthognathic surgery. *Maxillofac. Plast. Reconstr. Surg.* **2015**, *37*, 6. [CrossRef]
10. Islam, O.; Soboleski, D.; Symons, S.; Davidson, L.K.; Ashworth, M.A.; Babyn, P. Development and duration of radiographic signs of bone healing in children. *Am. J. Roentgenol.* **2000**, *175*, 75–78. [CrossRef]
11. Böstman, O.; Pihlajamäki, H.J.B. Clinical biocompatibility of biodegradable orthopaedic implants for internal fixation: A review. *Biomaterials* **2000**, *21*, 2615–2621. [CrossRef] [PubMed]
12. da Silva, D.; Kaduri, M.; Poley, M.; Adir, O.; Krinsky, N.; Shainsky-Roitman, J.; Schroeder, A. Biocompatibility, biodegradation and excretion of polylactic acid (PLA) in medical implants and theranostic systems. *Chem. Eng. J.* **2018**, *340*, 9–14. [CrossRef] [PubMed]
13. Fukushima, K.; Hirata, M.; Kimura, Y.J.M. Synthesis and characterization of stereoblock poly (lactic acid) s with nonequivalent D/L sequence ratios. *Macromolecules* **2007**, *40*, 3049–3055. [CrossRef]
14. Xinteng, Z.; Weisan, P.; Ruhua, Z.; Feng, Z.J.D.P. Preparation and evaluation of poly (D, L-lactic acid)(PLA) or D, L-lactide/glycolide copolymer (PLGA) microspheres with estradiol. *Die Pharm.* **2002**, *57*, 695–697.
15. Jamshidian, M.; Tehrany, E.A.; Imran, M.; Jacquot, M.; Desobry, S. Poly-lactic acid: Production, applications, nanocomposites, and release studies. *Compr. Rev. Food Sci. Food Saf.* **2010**, *9*, 552–571. [CrossRef] [PubMed]
16. Pitt, G.; Gratzl, M.; Kimmel, G.; Surles, J.; Sohindler, A.J.B. Aliphatic polyesters II. The degradation of poly (DL-lactide), poly (ε-caprolactone), and their copolymers in vivo. *Biomaterials* **1981**, *2*, 215–220. [CrossRef] [PubMed]
17. Grizzi, I.; Garreau, H.; Li, S.; Vert, M.J.B. Hydrolytic degradation of devices based on poly (DL-lactic acid) size-dependence. *Biomaterials* **1995**, *16*, 305–311. [CrossRef]
18. De Jong, W.H.; Eelco Bergsma, J.; Robinson, J.E.; Bos, R.R.M. Tissue response to partially in vitro predegraded poly-L-lactide implants. *Biomaterials* **2005**, *26*, 1781–1791. [CrossRef]
19. Mohapatra, A.K.; Mohanty, S.; Nayak, S.K. Effect of PEG on PLA/PEG blend and its nanocomposites: A study of thermo-mechanical and morphological characterization. *Polym. Compos.* **2014**, *35*, 283–293. [CrossRef]

20. Reis, M.O.; Olivato, J.B.; Bilck, A.P.; Zanela, J.; Grossmann MV, E.; Yamashita, F. Biodegradable trays of thermoplastic starch/poly (lactic acid) coated with beeswax. *Ind. Crops Prod.* **2018**, *112*, 481–487. [CrossRef]
21. DeStefano, V.; Khan, S.; Tabada, A. Applications of PLA in modern medicine. *Eng. Regen.* **2020**, *1*, 76–87. [CrossRef]
22. Gutiérrez-Sánchez, M.; Escobar-Barrios, V.A.; Pozos-Guillén, A.; Escobar-García, D.M. RGD-functionalization of PLA/starch scaffolds obtained by electrospinning and evaluated in vitro for potential bone regeneration. *Mater. Sci. Eng. C* **2019**, *96*, 798–806. [CrossRef] [PubMed]
23. García, N.L.; Lamanna, M.; D'Accorso, N.; Dufresne, A.; Aranguren, M.; Goyanes, S. Biodegradable materials from grafting of modified PLA onto starch nanocrystals. *Polym. Degrad. Stab.* **2012**, *97*, 2021–2026. [CrossRef]
24. Diyana, Z.N.; Jumaidin, R.; Selamat, M.Z.; Ghazali, I.; Julmohammad, N.; Huda, N.; Ilyas, R.A. Physical Properties of Thermoplastic Starch Derived from Natural Resources and Its Blends: A Review. *Polymers* **2021**, *13*, 1396. [CrossRef] [PubMed]
25. Rahman, M.; Hamdan, S.; Baini, R.; Bakri, M.K.; Muhammad, A.; Law Nyuk Khui, P.; Kakar, A.; Sanaullah, K. Chemically Treated Borneo Sago (Metroxylon sagu) Starch Reinforced Poly Lactic Acid Bio-composites. *Bioresources* **2020**, *15*, 1641–1655. [CrossRef]
26. Umas, R.A.; Supriadi, S.; Whulanza, Y.; Hasan, A.A.A.F. Mechanical strength comparison study of biodegradable materials for miniplate implant using finite element analysis. *AIP Conf. Proc.* **2023**, *2571*, 030001.
27. Whulanza, Y.; Azadi, A.; Supriadi, S.; Rahman, S.F.; Chalid, M.; Irsyad, M.; Nadhif, M.H.; Kreshanti, P. Tailoring mechanical properties and degradation rate of maxillofacial implant based on sago starch/polylactid acid blend. *Heliyon* **2022**, *8*, e08600. [CrossRef]
28. Misman, M.A.; Azura, A.R.; Hamid, Z.A.A. The Effect of Acrylonitrile Concentration on Starch Grafted Acrylonitrile (ANS) Stability in Carboxylated Nitrile Butadiene Rubber (XNBR) Latex. *Procedia Chem.* **2016**, *19*, 770–775. [CrossRef]
29. Wu, C.S. Improving polylactide/starch biocomposites by grafting polylactide with acrylic acid—Characterization and biodegradability assessment. *Macromol. Biosci.* **2005**, *5*, 352–361. [CrossRef]
30. Casalini, T.; Rossi, F.; Castrovinci, A.; Perale, G. A Perspective on Polylactic Acid-Based Polymers Use for Nanoparticles Synthesis and Applications. *Front. Bioeng. Biotechnol.* **2019**, *7*, 259. [CrossRef]
31. Kumar, R.; Alex, Y.; Nayak, B.; Mohanty, S. Effect of poly (ethylene glycol) on 3D printed PLA/PEG blend: A study of physical, mechanical characterization and printability assessment. *J. Mech. Behav. Biomed. Mater.* **2023**, *141*, 105813. [CrossRef]
32. Yew, G.H.; Mohd Yusof, A.M.; Mohd Ishak, Z.A.; Ishiaku, U.S. Water absorption and enzymatic degradation of poly(lactic acid)/rice starch composites. *Polym. Degrad. Stab.* **2005**, *90*, 488–500. [CrossRef]
33. Raj, S.A.; Muthukumaran, E.; Jayakrishna, K. A Case Study of 3D Printed PLA and Its Mechanical Properties. *Mater. Today Proc.* **2018**, *5*, 11219–11226. [CrossRef]
34. Nugroho, A.; Ardiansyah, R.; Rusita, L.; Larasati, I.L. Effect of layer thickness on flexural properties of PLA (PolyLactid Acid) by 3D printing. *J. Phys. Conf. Ser.* **2018**, *1130*, 012017. [CrossRef]
35. *ISO 10993-5*; Biological Evaluation of Medical Devices, Part 5: Tests for In Vitro Cytotoxicity. ISO (International Organization for Standardization): Geneva, Switzerland, 2009.
36. Kim, C.-H.; Kim, D.-W.; Cho, K.Y. The influence of PEG molecular weight on the structural changes of corn starch in a starch/PEG blend. *Polym. Bull.* **2009**, *63*, 91–99. [CrossRef]
37. Li, D.; Jiang, Y.; Lv, S.; Liu, X.; Gu, J.; Chen, Q.; Zhang, Y. Preparation of plasticized poly (lactic acid) and its influence on the properties of composite materials. *PLoS ONE* **2018**, *13*, e0193520. [CrossRef] [PubMed]
38. Ferrarezi, M.M.F.; Oliveira Taipina, M.; Escobar da Silva, L.C.; Gonçalves, M.D.C. Poly(Ethylene Glycol) as a Compatibilizer for Poly(Lactic Acid)/Thermoplastic Starch Blends. *J. Polym. Environ.* **2013**, *21*, 151–159. [CrossRef]
39. Akrami, M.; Ghasemi, I.; Azizi, H.; Karrabi, M.; Seyedabadi, M. A new approach in compatibilization of the poly(lactic acid)/thermoplastic starch (PLA/TPS) blends. *Carbohydr. Polym.* **2016**, *144*, 254–262. [CrossRef]
40. Park, J.W.; Im, S.S.; Kim, S.H.; Kim, Y.H. Biodegradable polymer blends of poly(L-lactic acid) and gelatinized starch. *Polym. Eng. Sci.* **2000**, *40*, 2539–2550. [CrossRef]
41. Rogovina, S.Z.; Aleksanyan, K.V.; Loginova, A.A.; Ivanushkina, N.E.; Vladimirov, L.V.; Prut, E.V.; Berlin, A.A. Influence of PEG on Mechanical Properties and Biodegradability of Composites Based on PLA and Starch. *Starch-Stärke* **2018**, *70*, 1700268. [CrossRef]
42. Yu, Y.; Cheng, Y.; Ren, J.; Cao, E.; Fu, X.; Guo, W. Plasticizing effect of poly(ethylene glycol)s with different molecular weights in poly(lactic acid)/starch blends. *J. Appl. Polym. Sci.* **2015**, *132*, 41808. [CrossRef]
43. Bhiogade, A.; Kannan, M.; Devanathan, S. Degradation kinetics study of Poly lactic acid(PLA) based biodegradable green composites. *Mater. Today Proc.* **2020**, *24*, 806–814. [CrossRef]
44. Mikos, A.G.; Thorsen, A.J.; Czerwonka, L.A.; Bao, Y.; Langer, R.; Winslow, D.N.; Vacanti, J.P.J.P. Preparation and characterization of poly (L-lactic acid) foams. *Polymer* **1994**, *35*, 1068–1077. [CrossRef]
45. Reed, A.; Gilding, D.J.P. Biodegradable polymers for use in surgery—Poly (glycolic)/poly (Iactic acid) homo and copolymers: 2. In vitro degradation. *Polymer* **1981**, *22*, 494–498. [CrossRef]
46. Xu, L.; Crawford, K.; Gorman, C.B.J.M. Effects of temperature and pH on the degradation of poly (lactic acid) brushes. *Macromolecules* **2011**, *44*, 4777–4782. [CrossRef]
47. Murariu, M.; Dubois, P. PLA composites: From production to properties. *Adv. Drug Deliv. Rev.* **2016**, *107*, 17–46. [CrossRef]
48. Saragih, A.S.; Pradipta, R.S.; Supriadi, S.; Chalid, M.; Whulanza, Y. Mold design and simulation of polymer miniplate and screw implant in the micro injection molding. *AIP Conf. Proc.* **2023**, *2837*, 040008.

49. Supriadi, S.; Whulanza, Y. TiBio teaching industry: Research based product development in the case of medical degradable implant. *AIP Conf. Proc.* **2023**, *2536*, 040012.
50. Chalid, M.; Gustiraharjo, G.; Pangesty, A.-I.; Adyandra, A.; Whulanza, Y.; Supriadi, S. Effect of PEG Incorporation on Physico-chemical and in vitro Degradation of PLLA/PDLLA Blends: Application in Biodegradable Implants. *J. Renew. Mater.* **2023**, *11*, 3043–3056. [CrossRef]
51. Liu, H.; Zhang, J. Research progress in toughening modification of poly(lactic acid). *J. Polym. Sci. Part B Polym. Phys.* **2011**, *49*, 1051–1083. [CrossRef]
52. Gamage, A.; Liyanapathiranage, A.; Manamperi, A.; Gunathilake, C.; Mani, S.; Merah, O.; Madhujith, T. Applications of Starch Biopolymers for a Sustainable Modern Agriculture. *Sustainability* **2022**, *14*, 6085. [CrossRef]
53. Awale, R.J.; Ali, F.B.; Azmi, A.S.; Puad, N.I.M.; Anuar, H.; Hassan, A. Enhanced Flexibility of Biodegradable Polylactic Acid/Starch Blends Using Epoxidized Palm Oil as Plasticizer. *Polymers* **2018**, *10*, 977. [CrossRef]
54. Kozlowski, M.; Masirek, R.; Piorkowska, E.; Gazicki-Lipman, M. Biodegradable blends of poly(L-lactide) and starch. *J. Appl. Polym. Sci.* **2007**, *105*, 269–277. [CrossRef]
55. Su, Q.; Qiao, Y.; Xiao, Y.; Yang, S.; Wu, H.; Li, J.; He, X.; Hu, X.; Yang, H.; Yong, X. Research progress of 3D printed poly (ether ether ketone) in the reconstruction of craniomaxillofacial bone defects. *Front. Bioeng. Biotechnol.* **2023**, *11*, 1259696. [CrossRef]
56. Zhang, T.; Wang, W.; Liu, J.; Wang, L.; Tang, Y.; Wang, K. A review on magnesium alloys for biomedical applications. *Front. Bioeng. Biotechnol.* **2022**, *10*, 953344. [CrossRef]